New U-Pb zircon dates from the Aishihik batholith, southern Yukon

N.L. Joyce
Geological Survey of Canada, Ottawa, ON

M. Colpron[1]
Yukon Geological Survey

M.M. Allan
Mineral Deposit Research Unit, University of British Columbia

P.J. Sack
Yukon Geological Survey

J.L. Crowley
Isotope Geology Laboratory, Boise State University, Boise, ID

J.B. Chapman
Geological Survey of Canada, Vancouver, BC

Joyce, N.L., Colpron, M., Allan, M.M., Sack, P.J., Crowley, J.L and Chapman, J.B., 2016. New U-Pb zircon dates from the Aishihik batholith, southern Yukon. *In:* Yukon Exploration and Geology 2015, K.E. MacFarlane and M.G. Nordling (eds.), Yukon Geological Survey, p. 131-149, plus digital appendices.

ABSTRACT

New U-Pb zircon dates (SHRIMP and LA-ICPMS) from granitoid rocks of the Aishihik batholith indicate a range of *ca.* 190-180 Ma for the Long Lake plutonic suite, as previously indicated by less precise, multi-grain TIMS dates. None of the phases in the Aishihik batholith are as old as the Minto suite to the north, therefore limiting the potential for Minto-style Cu-Au-Ag mineralization in the batholith. However, local occurrences of apparently shallow-level intrusions suggest that parts of the Aishihik batholith may present suitable targets for more typical porphyry Cu-Au mineralization. LA-ICPMS U-Pb zircon dating of two orthogneiss samples from the western margin of the Aishihik batholith yielded Early Mississippian protolith ages akin to the Simpson Range plutonic suite (Yukon-Tanana terrane), and Jurassic overgrowths consistent with partial melting related to intrusion of the Aishihik batholith.

[1]*maurice.colpron@gov.yk.ca*

INTRODUCTION

The Aishihik batholith is one of a series of large, composite Late Triassic to Early Jurassic granitoid batholiths that intrude the Intermontane terranes in southern Yukon (Fig. 1). These plutons form the northern extension of a pair of plutonic belts related to arc magmatism of Stikinia and Quesnellia in British Columbia, where they are associated with a number of significant Cu-Au(Mo) porphyry deposits (Logan and Mihalynuk, 2014). The BC porphyry deposits are typically large tonnage, low grade and formed at shallow crustal levels. In Yukon, high-grade (but low tonnage) Cu-Au-Ag mineralization is locally hosted in latest Triassic-Early Jurassic plutons (*e.g.*, Minto, Carmacks Copper), but the style of mineralization is not typical of porphyry deposits. All indications are that the Yukon deposits either formed, or were deformed, at mid-crustal levels during emplacement of the latest Triassic-earliest Jurassic plutons (*e.g.*, Tafti, 2005; Hood, 2012). These plutons and associated mineralization were emplaced prior to, or during accretion of the Intermontane terranes to western North America and the onset of Cordilleran orogenesis (*e.g.*, Nelson *et al.*, 2013; Logan and Mihalynuk, 2014; Colpron *et al.*, 2015). To date, Minto-style mineralization has only been confirmed in a relatively restricted area northwest of Carmacks, commonly referred to as the Carmacks Copper belt, despite the fact that plutons inferred to be coeval with the Granite Mountain and Minto plutons (which host the Carmacks Copper and Minto deposits, respectively) are much more extensive in southern Yukon.

Despite the economic importance of the Late Triassic-Early Jurassic plutons, they have so far received little attention in Yukon and as a result they generally remain poorly characterized. Previous studies focused primarily on areas known to host mineralization (*e.g.*, Tafti, 2005; Hood, 2012). Regionally, the Late Triassic-Early Jurassic plutons were locally characterized as part of regional mapping programs (*e.g.*, Gordey and Stevens, 1994; Johnston *et al.*, 1996; Colpron *et al.*, 2002; Gordey and Ryan, 2005). These programs produced some U-Pb dates and geochemical data for the plutons, but no attempts were made at understanding their petrogenesis, locally or regionally.

In 2014, the Yukon Geological Survey embarked on a regional study of Late Triassic to Jurassic magmatism in Yukon in order to fill this knowledge gap. This program aims at developing a standardized, modern and high-quality geochronological, geochemical and isotopic dataset for Late Triassic to Jurassic plutons in Yukon in order to elucidate the regional petrogenesis of these magmatic belts. Specific objectives are to identify other plutons with potential to host Minto-style Cu-Au-Ag mineralization, and to evaluate the potential for Early Jurassic plutons in Yukon to host porphyry Cu-Au mineralization.

In this contribution, we report new U-Pb zircon dates from eight samples collected during regional reconnaissance of the Aishihik batholith. These results add to previously published Thermal Ionization Mass Spectrometry (TIMS) dates (Johnston *et al.*, 1996; Hart, 1997; Table 1; Fig. 2) which were obtained by analyzing multi-grain zircon fractions, and generally yielded discordant dates attributed to either inheritance or lead-loss. Most of the new analyses presented in this paper were obtained by *in-situ* spot analyses of zircon using either Sensitive High Resolution Ion Microprobe (SHRIMP) or Laser Ablation-Inductively Coupled Plasma Mass Spectrometry (LA-ICPMS), coupled with Scanning Electron Microscope (SEM) based imaging, thereby permitting better spatial resolution of the different age components.

LATE TRIASSIC - JURASSIC PLUTONIC SUITES IN YUKON

Late Triassic to Jurassic plutons in Yukon are grouped into four distinct plutonic suites: 1) the Late Triassic Stikine suite; 2) the latest Triassic to Early Jurassic Minto suite (formerly Klotassin and/or Aishihik suite; *see* discussion below); 3) the Early Jurassic Long Lake suite; and 4) the Middle Jurassic Bennett-Bryde suite (following subdivisions of Woodsworth *et al.*, 1991; Gordey and Makepeace, 2001; Colpron *et al.*, 2016). Only the Minto and Long Lake suites will be discussed in this paper, as both were previously considered to comprise the Aishihik batholith (Tempelman-Kluit, 1974; Woodsworth *et al.*, 1991; Johnston and Erdmer, 1995; Johnston *et al.*, 1996).

The Late Triassic-Early Jurassic suite of mainly granodiorite plutons, including the Minto, Granite Mountain, Tatchun, Lokken and part of the Aishihik batholith (Fig. 1), was originally thought to extend to the western Dawson Range and include the Klotassin batholith (Tempelman-Kluit, 1974, 1984, 2009; Tempelman-Kluit and Wanless, 1975). The suite was named the Klotassin suite and presumed to be of Late Triassic age (Tempelman-Kluit and Wanless, 1975; Woodsworth *et al.*, 1991). However, subsequent K-Ar and U-Pb dating of the Klotassin suite in the Dawson Range indicated a mid-Cretaceous age for the former

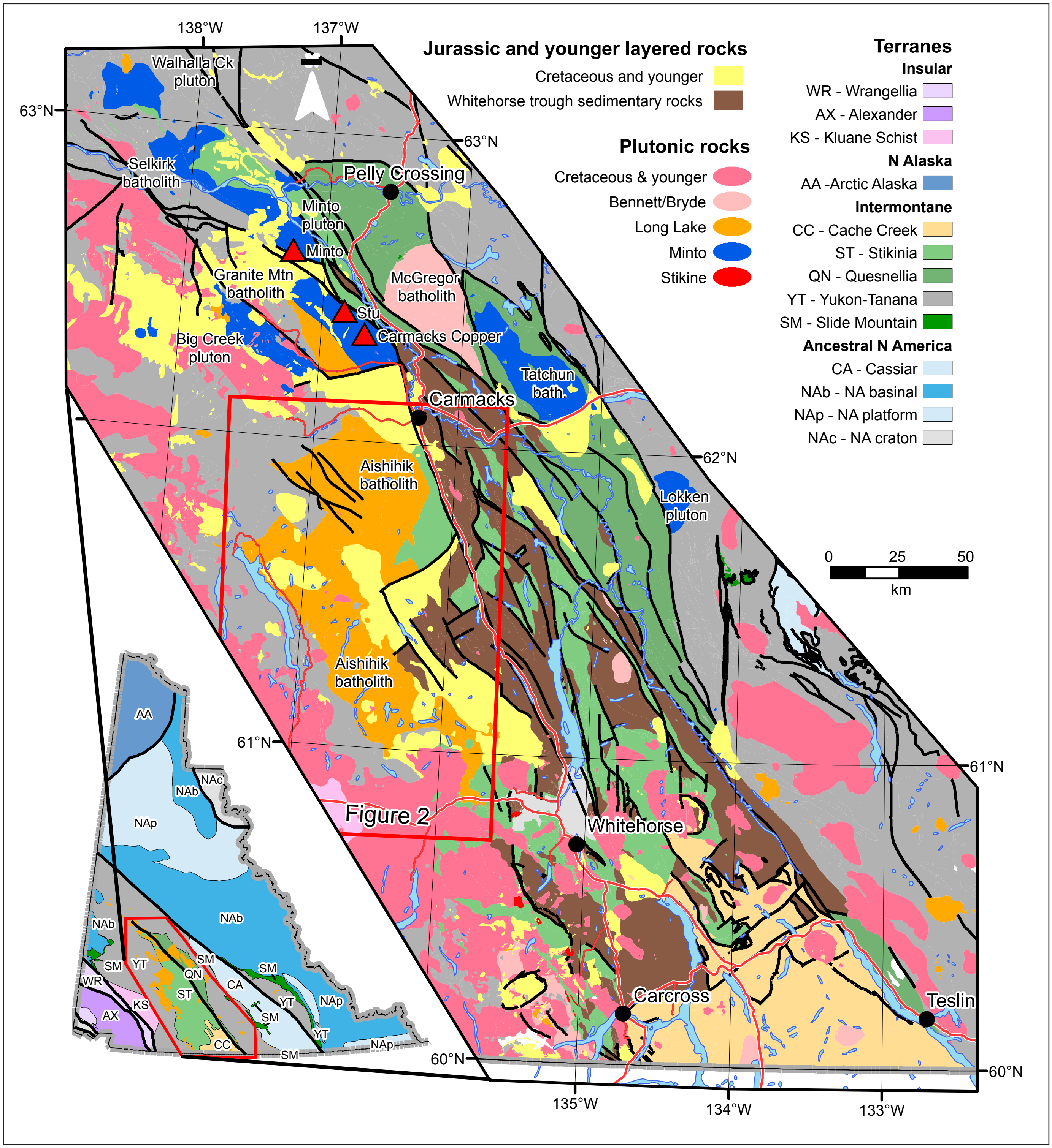

Figure 1. *Terrane map (Colpron and Nelson, 2011) and regional geology of southern Yukon (www.geology.gov.yk.ca/update_yukon_bedrock_geology_map.html). Main map coloured by terrane with Whitehorse trough and younger cover sequences shown in brown and yellow, respectively. Late Triassic to Jurassic plutonic rocks are subdivided into 4 suites as described in text. Inset Yukon terrane map to lower left shows the area of the main map; note that all Late Triassic to Jurassic plutonic rocks are shown in orange in the inset map.*

Klotassin batholith (*ca.* 100 Ma; now known as the Dawson Range batholith; Godwin, 1975; Breitsprecher and Mortensen, 2004). This led Johnston and Erdmer (1995) to abandon the name Klotassin suite and rename presumed Early Jurassic granodiorite as the Aishihik suite (*ca.* 186 Ma; Johnston *et al.*, 1996). Granodiorite of the Aishihik batholith is intruded by 'younger', more felsic quartz monzonite and granite of the Long Lake suite (pink quartz monzonite of Tempelman-Kluit, 1974; Woodsworth *et al.*, 1991; Johnston and Erdmer, 1995) that also yielded a *ca.* 186 Ma date (Johnston *et al.*, 1996).

Further studies of the Minto, Granite Mountain, Big Creek and Tatchun plutons indicated U-Pb zircon ages ranging from *ca.* 204-196 Ma (Tafti, 2005; Hood, 2012; Colpron, 2011; Breitsprecher and Mortensen, 2004), restoring a Late Triassic to Early Jurassic age range for the Aishihik suite. The suite has important economic significance because it hosts Cu-Au-Ag mineralization at the Minto and Carmacks Copper (formerly Williams Creek) deposits (Fig. 1; Tafti, 2005; Hood, 2012). We present below new U-Pb data suggesting that none of the granodiorite phases in the Aishihik batholith are as old as the Minto, Granite Mountain and Tatchun plutons (which became archetypical examples of the Aishihik suite). Hence, assignment of these older plutons to the Aishihik suite no longer seems appropriate. Instead, we propose assignment of the Late Triassic-Early Jurassic granodiorite plutons to the newly defined Minto plutonic suite (*e.g.*, Colpron *et al.*, 2016).

Table 1. *Summary of dates from Aishihik batholith.*

Sample	Date		Error (2 σ)	MSWD	Lithology	Mineral dated	Comment	Latitude	Longitude	Reference
CDB10-102	182	±	2	1.2	porphyritic granite	zircon	SHRIMP - weighted mean of 9 analyses	61.22232	-136.28342	this study
CDB10-103	181	±	2	1.4	quartz monzonite	zircon	SHRIMP - weighted mean of 7 analyses	61.36263	-136.59095	this study
CDB10-105	188	±	2	1.3	hbl-bt granodiorite	zircon	SHRIMP - weighted mean of 9 analyses	61.64177	-136.7876	this study
CDB10-106	183	±	2	1.4	porphyritic granodiorite	zircon	SHRIMP - weighted mean of 15 analyses	61.89086	-136.77289	this study
CDB10-107	187	±	2	1.4	hbl-bt tonalite	zircon	SHRIMP - weighted mean of 12 analyses	61.79203	-136.28931	this study
10-SI-223	344	±	6		granodiorite orthogneiss	zircon	LA-ICPMS - weighted mean of 15 oldest zircons	61.44778	-137.06437	this study
	193	±	5			zircon	LA-ICPMS - weighted mean of 2 youngest zircons			this study
MA14-AB9	186	±	2	1.5	quartz porphyry	zircon	LA-ICPMS - weighted mean of 19 analyses	61.88169	-136.93544	this study
MA14-AB6	345	±	4	1.5	granodiorite orthogneiss	zircon	LA-ICPMS - weighted mean of 17 cores	61.91717	-137.21234	this study
	187	±	5	0.5		zircon	LA-ICPMS - weighted mean of 2 rims			this study
Previously published dates										
92CH-75-8	183	±	2		quartz monzonite	zircon	TIMS - 3 pt regression, lower intercept	60.93667	-135.80829	Hart (1997)
STJ86-82	185.6	±	2.4	0.5	quartz monzonite	zircon	TIMS - 5 pt regression, lower intercept	61.33336	-136.6781	Johnston et al. (1996)
STJ87-108	186.0	±	2.8		granodiorite	zircon	TIMS - mean age of two concordant fractions	61.55728	-137.3277	Johnston et al. (1996)
QM87-92	187.7	±	0.6		quartz monzonite	titanite	TIMS - mean age of two concordant fractions	61.69866	-136.27249	Johnston et al. (1996)
STJ-OG	352.3	±	2.4	0.2	granitic orthogneiss	zircon	TIMS - 3 pt regression, upper intercept	61.48042	-137.17689	Johnston et al. (1996)
	184.4	±	0.5			titanite	TIMS - most precise of 2 concordant analyses			Johnston et al. (1996)

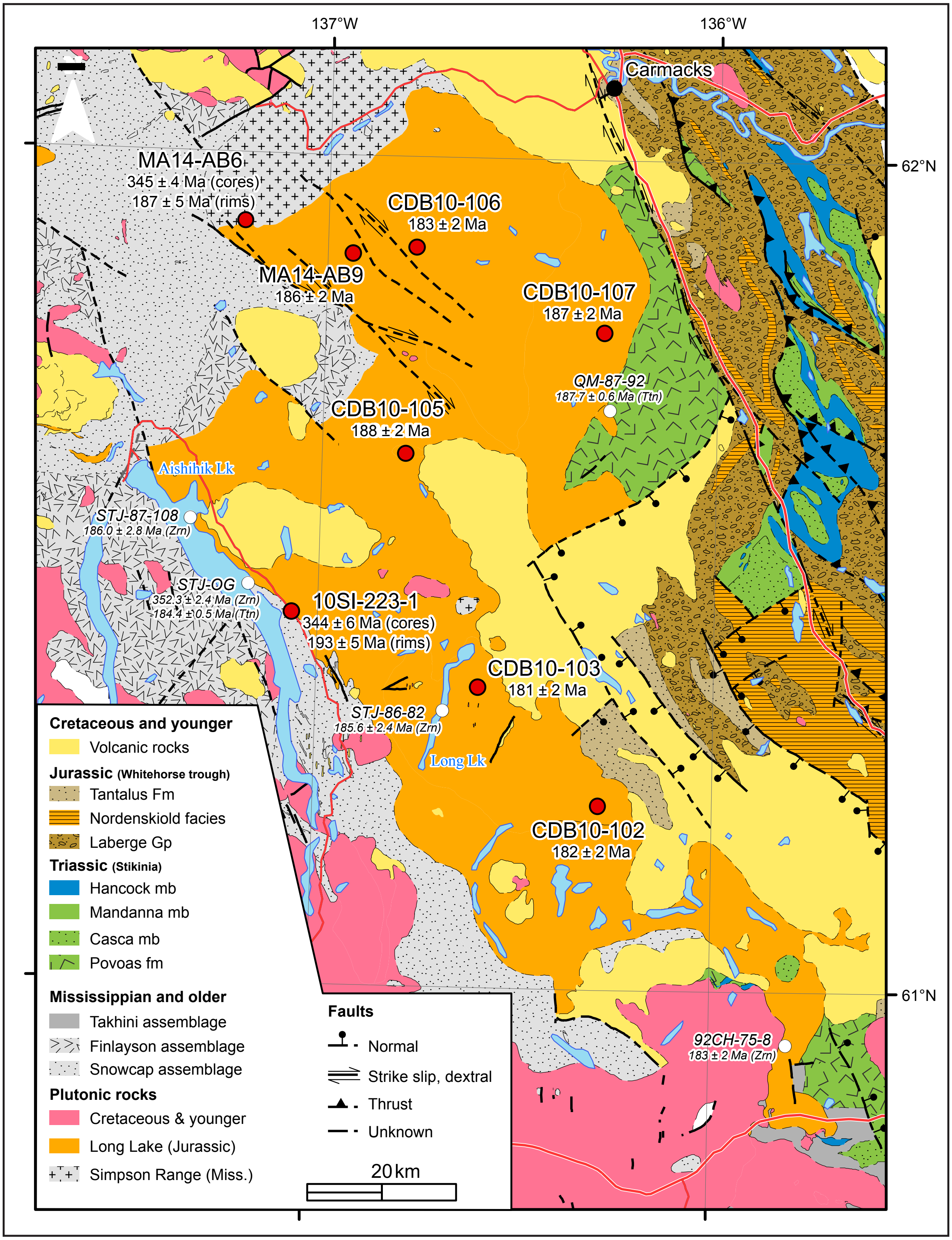

Figure 2. *Geological map of the area surrounding the Aishihik batholith (geology from www.geology.gov.yk.ca/update_yukon_bedrock_geology_map.html). Geology is coloured by terrane affinity with patterns showing regional units. Red circles are geochronology samples reported in this paper; small white circles show location of previous geochronology samples (see Table 1 for details).*

AISHIHIK BATHOLITH

The Aishihik batholith is the largest of the Late Triassic-Early Jurassic composite plutons in Yukon (Fig. 1). It extends from near Whitehorse to the vicinity of Carmacks, and intrudes strata of Stikinia and Yukon-Tanana terranes west of the Whitehorse trough (Figs. 1 and 2). The batholith comprises granitoid lithologies that range in compositions from quartz diorite, tonalite and granodiorite, to quartz monzonite and granite, with the various compositions mutually intermixed and with gradational contacts (Tempelman-Kluit, 1974; Johnston and Erdmer, 1995; Johnston *et al.*, 1996). Originally the name Aishihik batholith was primarily applied to rocks of granodioritic composition, and the two regions dominated by quartz monzonite and granitic compositions, near Long Lake and at the north end of the batholith near Carmacks, were referred to as the Long Lake and Carmacks batholiths, respectively (Tempelman-Kluit, 1974; Woodsworth *et al.*, 1991; Johnston and Erdmer, 1995). More recently, the entire area underlain by Jurassic granitoid rocks has been called the Aishihik batholith (Gordey and Makepeace, 2001; Colpron *et al.*, 2016), and this is the usage followed in this paper (Fig. 1).

Granodiorite and tonalite are the dominant intermediate compositions within the Aishihik batholith. They are generally medium to coarse-grained, equigranular to K-feldspar porphyritic, and typically contain hornblende and biotite, with hornblende commonly more abundant than biotite (Figs. 3a-c). Johnston and Erdmer (1995) reported occurrence of magmatic epidote from granodiorite of the Aishihik batholith; an observation that could not be replicated in our suite of samples. The presence of magmatic epidote is a key argument to suggest emplacement of the granodiorite-tonalite in the Aishihik batholith at >25 km depth (Johnston and Erdmer, 1995; Johnston *et al.*, 1996).

Quartz monzonite and granite of the Aishihik batholith are typically coarse-grained and K-feldspar porphyritic, and also commonly contain biotite and hornblende (Figs. 3d-e). The local abundance of large, pink K-feldspar phenocrysts led Tempelman-Kluit (1974) to assign the name of 'pink quartz monzonite' to these rocks (Fig. 3e). Occurrences of granite are commonly associated with late aplite and pegmatite dikes, local miarolitic cavities, and locally finer grained quartz porphyry (Figs. 3f). These more felsic, and apparently shallowly-emplaced rocks appear to be more common in (but not exclusive to) the northern part of the batholith (Fig. 2). The various compositions that make up the Aishihik batholith are variably intermixed with gradational internal contacts, though field relationships generally suggest that granodiorite-tonalite phases are older, and quartz monzonite-granite phases are relatively younger (Tempelman-Kluit, 1974; Johnston and Erdmer, 1995; Johnston *et al.*, 1996).

Johnston and Erdmer (1995, p. 67) described the rocks of the Aishihik batholith as "characteristically foliated". Although we observed weak to moderate foliation (both magmatic and solid state) in many locations throughout the batholith, for the most part granitoid rocks in the Aishihik batholith are undeformed (Figs. 3a-f). Johnston and Erdmer (1995, p. 75) further suggested that foliation intensity increased toward the western margin of the Aishihik batholith and was locally gneissic in character (their S_t fabric). Our observations, and the geochronological data we present below, indicate that the granodiorite gneiss at the western margin of the Aishihik batholith (Fig. 3g-h) is part of the Mississippian Simpson Range plutonic suite of the Yukon-Tanana terrane (*e.g.*, Mortensen, 1992; Colpron *et al.*, 2006). A series of late upright folds are superposed on the gneissic foliation and also fold the western intrusive contact of the batholith near Aishihik Lake (Israel and Borch, 2015).

Previous U-Pb geochronology of the Aishihik batholith is limited to multi-grain, generally discordant TIMS dates from five samples (Fig. 2). Johnston *et al.* (1996) reported a $^{207}Pb/^{206}Pb$ date of 186.0 ± 2.8 Ma for two concordant zircon fractions in a foliated granodiorite from the western part of the Aishihik batholith. A sample of quartz monzonite from Long Lake yielded a lower intercept U-Pb zircon date of 185.6 ± 2.4 Ma (Johnston *et al.*, 1996). Another sample of quartz monzonite yielded a $^{206}Pb/^{238}U$ titanite date of 187.7 ± 0.6 Ma (Johnston *et al.*, 1996). A quartz monzonite from the southern tail of the Aishihik batholith yielded a lower intercept U-Pb zircon date of 183 ± 2 Ma (Hart, 1997). Finally, a granitic orthogneiss from the western margin of the Aishihik batholith yielded an upper intercept U-Pb zircon date of 352.3 ± 2.4 Ma, considered the age of the protolith, and a titanite cooling date of 184.4 ± 0.5 Ma (Johnston *et al.*, 1996).

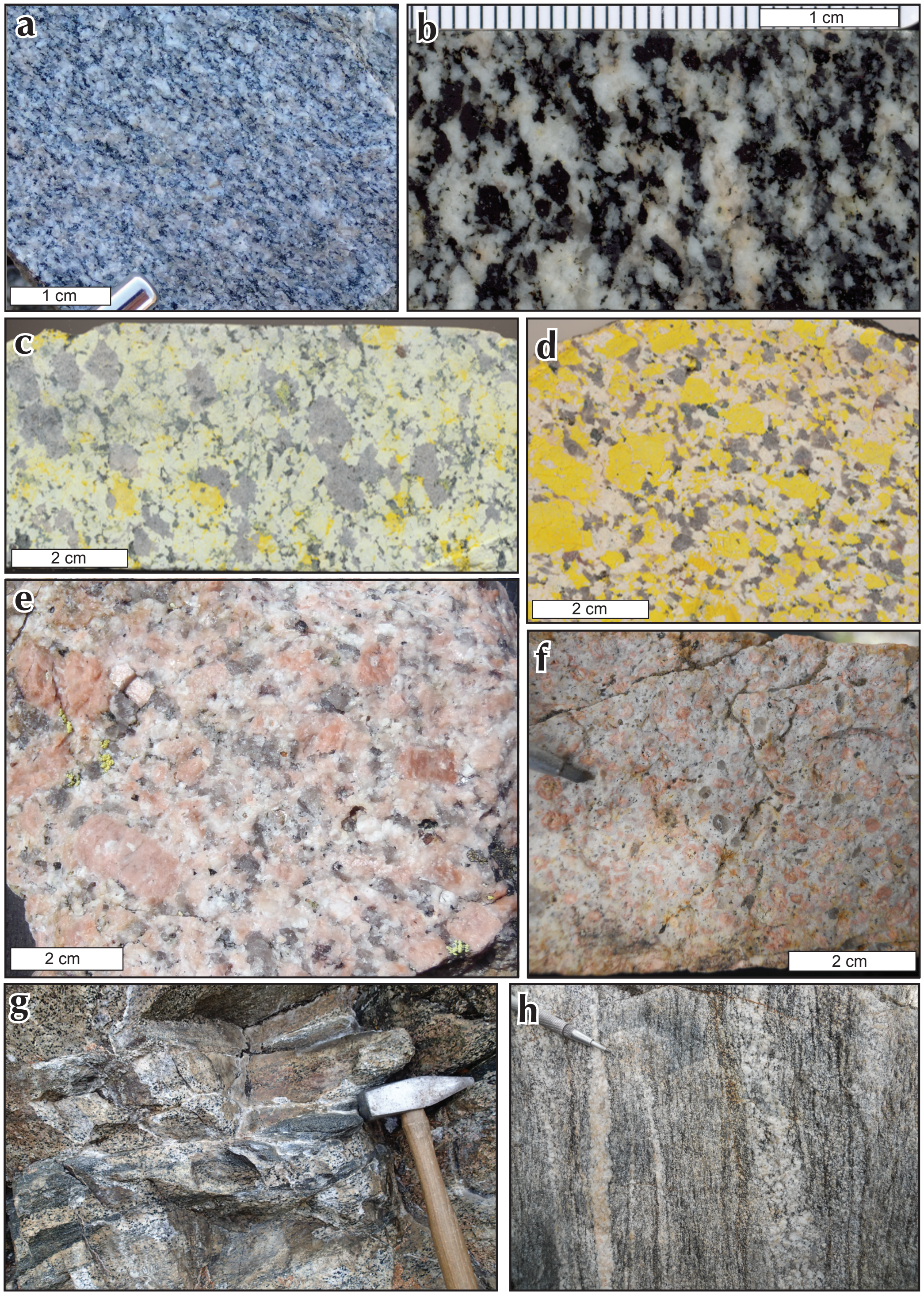

Figure 3. *Representative lithologies in the Aishihik batholith. (a) K-feldspar porphyritic granodiorite from central part of the batholith; (b) hornblende-biotite granodiorite at sample locality CDB-10-105; (c) stained slab of coarse-grained tonalite from the same locality as sample CDB-10-107. K-feldspar is stained yellow; (d) stained slab of K-feldspar porphyritic granite collected near sample CDB-10-103; (e) hand sample of K-feldspar porphyritic granite from station CDB-10-103. Note the large quartz phenocrysts characteristic of granite to quartz monzonite phases of the Aishihik batholith. (f) Weathered surface of quartz monzonite porphyry at location MA14-AB9. (g) Foliated, medium-grained, hornblende-biotite granodiorite with mafic schlieren at locality 10-SI-223; (h) sample of biotite granodiorite orthogneiss (MA14-AB6) from the northwestern margin of the Aishihik batholith.*

GEOCHRONOLOGY

In this contribution, we report new U-Pb zircon dates from eight samples collected during regional reconnaissance of the Aishihik batholith. Five samples were collected by J. Chapman and M. Colpron during a reconnaissance visit in August 2010. They were analyzed by N. Joyce using the Sensitive High Resolution Ion Microprobe (SHRIMP) at the Geological Survey of Canada laboratory in Ottawa (CDB-10-102, 103, 105, 106, 107; Table 1; analytical methods are given in Appendix 1 and data are presented in Appendix 2 and on Fig. 4). Sample 10-SI-223 was collected by S. Israel, M. Colpron and D. Murphy during a field visit of the Aishihik Lake area in September 2010 (Table 1). The sample was dated by J. Crowley using both Chemical Abrasion-Thermal Ionization Mass Spectrometry (CA-TIMS) and Laser Ablation-Inductively Coupled Plasma Mass Spectrometry (LA-ICPMS) at the Isotope Geology Laboratory at Boise State University (analytical methods detailed in Appendix 1; data are presented in Appendix 3 and 4, and on Fig. 5). Finally, samples MA14-AB6 and MA14-AB9 were collected by M. Allan during the early stages of our 2014 field studies. They were analyzed by LA-ICPMS at the Pacific Centre for Isotopic and Geochemical Research, University of British Columbia by M. Allan (analytical methods detailed in Appendix 1; data are presented in Appendix 5 and on Fig. 6). In general, these results confirm the ranges of dates previously obtained from multi-grain zircon fractions analyzed by TIMS (Table 1), but single-grain CA-TIMS analyses and the spatial resolution of laser and SHRIMP provide more accurate and precise results, circumventing problems of discordance in older TIMS ages caused by inheritance, post-crystallization Pb loss and mixing of age domains (Johnston *et al.*, 1996; Hart, 1997). Two of the samples (10-SI-223 and MA14-AB6) were collected from strongly foliated orthogneiss along the western margin of the Aishihik batholith (Fig. 2).

CDB-10-102 (Z11234) – PORPHYRITIC GRANITE

CDB-10-102 is a mafic-poor, K-feldspar porphyritic, coarse-grained, unfoliated, pink granite collected from the southern part of the Aishihik batholith (Fig. 2). The granite is characterized by large quartz phenocrysts (similar to Fig. 3e), and contains ~20% quartz, 30-35% plagioclase, 35-50% K-feldspar, and <10% hornblende. The granite is locally highly altered with fine Fe-oxide veinlets and extensive sericite and clay alteration of plagioclase relics.

Zircon grains recovered from this sample are 100-220 μm euhedral stubby prisms; results are shown in Figure 4a. In transmitted light the crystals are clear and colourless or pale yellow, and rarely contain inclusions. In both backscatter (BSE) and cathodo-luminescence (CL) scanning-electron microscope (SEM) images, the majority of the grains mounted for SHRIMP analysis show distinct oscillatory zoning. Cores were observed in about 15% of the grains. U content ranged between 181 and 456 ppm and Th/U values were moderate to high (0.37-0.85). Nine spots on individual grains returned a weighted mean $^{206}Pb/^{238}U$ date of 182 ± 2 Ma (mean square of weighted deviates [MSWD] = 1.2).

CDB-10-103 (Z11235) – QUARTZ MONZONITE

CDB-10-103 is a coarse-grained, unfoliated, biotite quartz monzonite collected from the top of Red Granite Mountain, near Long Lake (Fig. 2). It also has the 3-5 mm smokey quartz crystals characteristic of the more felsic compositions in the Aishihik batholith (Figs. 3d-e). Quartz makes up 19-30% of the rock, with 40-50% plagioclase, 15-31% K-feldspar, and up to 15% biotite. The plagioclase is commonly Fe-stained imparting a pink to red colouration to the weathered rock.

Zircon grains recovered from this sample are ~80-225 μm euhedral stubby prisms; results are shown in Figure 4b. In transmitted light the crystals are clear and colourless or pale yellow, and contain minor clear bubble-shaped inclusions. Cores, which have varying CL responses, are commonly sieve-textured in BSE, and are found in over 25% of the mounted grains. In both BSE and CL SEM images, the majority of the grains show distinct oscillatory zoning. Of the 16 analyses in Appendix 2, four are clearly from inherited zircons (Calibration 2; 197, 204, 361, and 1866 Ma). Dates of the 10 concordant analyses from Calibration 3 vary between 177 and 187 Ma, the weighted average of which is 182 Ma. The MSWD, however, is elevated at 3.3, suggesting more than one population is present. The weighted mean $^{206}Pb/^{238}U$ date of the 7 youngest analyses is 181 ± 2 Ma (MSWD = 1.4), which is interpreted as the crystallization age of the quartz monzonite. U content of this population of zircons ranged between 166 and 723 ppm, and Th/U values were moderate (0.16-0.37). Three analyses at ~187 Ma (grains 23, 46, and 47) are interpreted to be inherited from a slightly older intrusive phase. Grain 20 clearly has a *ca.* 197 Ma core mantled by a *ca.* 177 Ma rim (Fig. 4b).

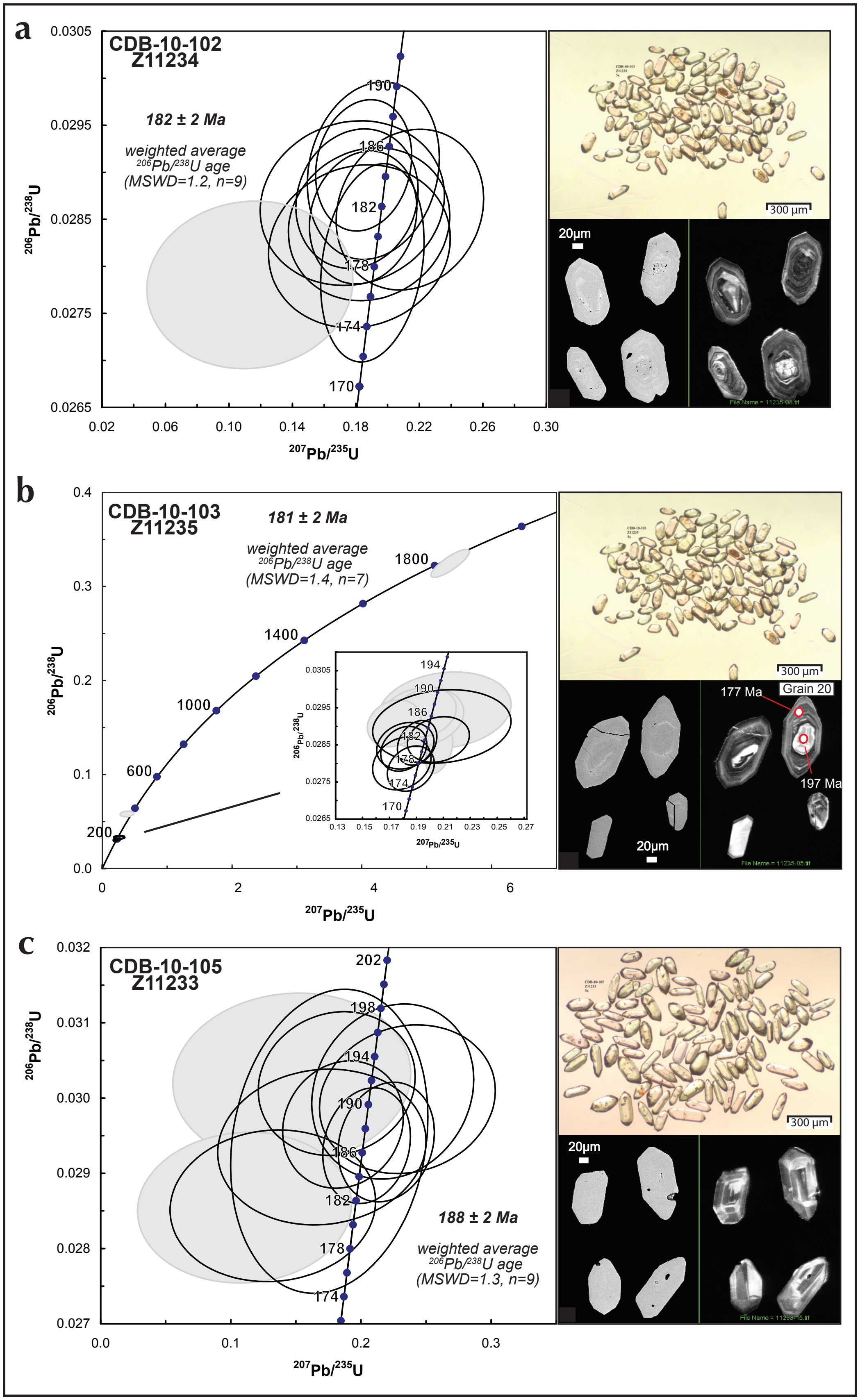

Figure 4. U-Pb concordia plots for five samples analyzed by SHRIMP methods at the Geological Survey of Canada geochronology laboratory in Ottawa. Each diagram consists of: a Concordia plot on the left, a photograph of zircon grains recovered in the upper right, and paired SEM backscatter (L) and CL images (R) in the lower right. Photograph of recovered grains shows the range in morphology, colour and size of zircons analyzed, and representative BSE and CL images show internal structure of the grains. For each Concordia plot, error ellipses are at the 2σ confidence level, unfilled ellipses are analyses used in calculating the mean weighted average age for each sample; light grey ellipses are analyses rejected from age calculations for reasons discussed in text.

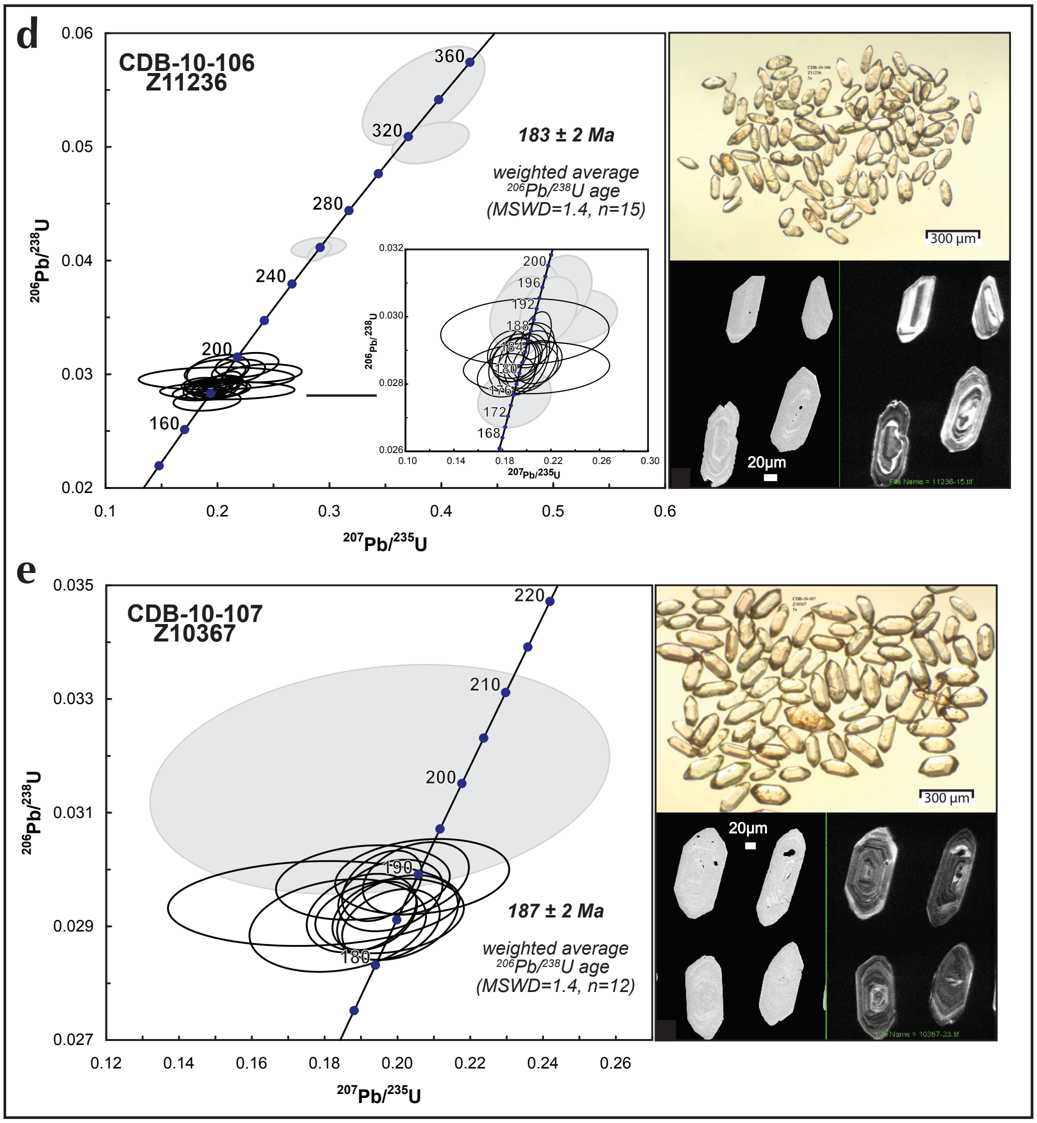

Figure 4 continued. *U-Pb concordia plots for five samples analyzed by SHRIMP methods at the Geological Survey of Canada geochronology laboratory in Ottawa. Each diagram consists of: a Concordia plot on the left, a photograph of zircon grains recovered in the upper right, and paired SEM backscatter (L) and CL images (R) in the lower right. Photograph of recovered grains shows the range in morphology, colour and size of zircons analyzed, and representative BSE and CL images show internal structure of the grains. For each Concordia plot, error ellipses are at the 2σ confidence level, unfilled ellipses are analyses used in calculating the mean weighted average age for each sample; light grey ellipses are analyses rejected from age calculations for reasons discussed in text.*

CDB-10-105 (Z11233) - WEAKLY FOLIATED HORNBLENDE-BIOTITE GRANODIORITE

CDB-10-105 is a mafic-rich, weakly foliated, medium-grained, equigranular hornblende-biotite granodiorite from the central part of the Aishihik batholith (Figs. 2 and 3b). It contains 15-25% fine-grained quartz, 35-50% plagioclase, 5-25% K-feldspar, up to 35% hornblende and 10% biotite. The weak magmatic foliation is shown by crude alignment of mafic minerals. Mafic minerals are locally altered to chlorite and epidote, with biotite more commonly altered.

Zircon grains recovered from this sample are 150-250 µm in size, stubby to elongate euhedral prisms; results are shown in Figure 4c. In transmitted light the crystals are clear and colourless or pale yellow, and commonly contain clear bubble or rod-shaped inclusions. Backscatter SEM images of the grains mounted for SHRIMP analysis reveal few internal textures of the grains, with the exception of inclusions and fractures. In CL, the majority of grains exhibit c-axis-parallel, broadly banded or striped zoning patterns, mantled by variably developed oscillatory-zoned growth (up to ~20 µm thick). Faint sector zoning is visible in grains polished normal to the c-axis. U content ranged between 130 and 245 ppm and Th/U values were moderate (0.36-0.68; Appendix 2). Cores were seen in only two of the grains. Nine spots on individual grains returned a weighted mean $^{206}Pb/^{238}U$ date of 188 ± 2 Ma (MSWD = 1.3). A 196 Ma date obtained for grain 85 is considered to reflect an inherited component (Appendix 2).

CDB-10-106 (Z11236) – PORPHYRITIC GRANODIORITE

CDB-10-106 is a coarse-grained, variably K-feldspar porphyritic, quartz-phyric hornblende (±biotite) granodiorite from Buffalo Mountain in the northern part of the Aishihik batholith (formerly the Carmacks batholith of Tempelman-Kluit, 1974; Johnston and Erdmer, 1995). Smokey quartz phenocrysts are up to 4 mm, in a 0.5-2 mm groundmass, as commonly noted in other quartz-rich rocks to the south, near Long Lake (*e.g.*, CDB-10-102 and 103; Figs. 2 and 3d). Quartz makes up 25-35% of the rock, with 40-50% plagioclase, 7-20% K-feldspar, and up to 10-15% hornblende (±biotite). The granodiorite is fresh and unfoliated.

Zircon grains recovered from this sample are ~90-225 μm stubby to elongate euhedral prisms; results are shown Figure 4d. In transmitted light the crystals are clear and colourless or pale yellow, and contain minor bubble-shaped clear inclusions. In both BSE and CL SEM images, the majority of the grains mounted for SHRIMP analysis show distinct oscillatory zoning. Cores were observed in about 20% of the grains. U content for the igneous grains ranged between 114 and 701 ppm and Th/U values were moderate (0.26-0.51; Appendix 2). Fifteen spots on individual grains returned a weighted mean $^{206}Pb/^{238}U$ date of 183±2 Ma (MSWD=1.4). Because the core regions of the grains in this sample were the largest and easiest to analyze, more analyses were carried out on this sample compared to the other four to characterize the inheritance profile of the Aishihik batholith. Eight inherited cores were analyzed, yielding dates of *ca.* 190, 260, 316 and 343 Ma (Appendix 2).

CDB-10-107 (Z10367) - HORNBLENDE-BIOTITE TONALITE

CDB-10-107 is a medium-grained, equigranular, hornblende-biotite tonalite to granodiorite collected from the northeastern portion of the Aishihik batholith (Figs. 2 and 3c). The rock contains up to 25% mafic minerals (hornblende and biotite), 35-55% plagioclase, 5-15% K-feldspar, and 25-40% quartz, but lacks the distinctive smokey-grey quartz phenocrysts characteristic of more felsic compositions to the west and south (*e.g.,* CDB-10-102, 103 and 106). A weak (magmatic) alignment of mafic minerals is locally apparent. Secondary epidote and titanite are locally important accessory phases.

Zircon grains recovered from this sample are ~100-300 μm stubby to slightly elongate euhedral prisms; results are shown in Figure 4e. In transmitted light the crystals are clear and colourless, and contain clear minor bubble and rod-shaped inclusions. In both BSE and CL SEM images, the majority of the grains mounted for SHRIMP analysis show distinct oscillatory zoning. Cores were observed in about 15% of the grains. U content for the igneous grains ranged between 234 and 826 ppm and Th/U values were moderate (0.34-0.64; Appendix 2). Twelve spots on individual grains returned a weighted mean $^{206}Pb/^{238}U$ date of 187±2 Ma (MSWD=1.4).

10-SI-223 - GRANODIORITE GNEISS

Sample 10-SI-223 is a strongly foliated, hornblende-biotite granodiorite to quartz diorite gneiss from the western margin of the Aishihik batholith, near the eastern shore of Aishihik Lake (Fig. 2). The rock is medium-grained with hornblende and biotite-rich schlieren (Fig. 3g)

Zircon is CL dark with weak to moderate sector and oscillatory zoning (Fig. 5 and Appendix 6). One third of the grains exhibit CL bright cores that were avoided during selection of grains for dating using the CA-TIMS method. Most grains have rims a few microns wide that grew after a period of zircon dissolution. CA-TIMS analyses (Fig. 5a and Appendix 3) form a discordant array nearly parallel to concordia that indicates the zircon is a mixture of two ages, 357±5 and 208±26 Ma (Fig. 5a).

The *in-situ* LA-ICPMS method was then performed to better resolve the age components (Appendix 4 and Fig. 5b). LA-ICPMS analyses show a similar spread of dates as seen in CA-TIMS analyses. The 15 oldest dates are equivalent, with a weighted mean date of 344±6 Ma (Fig. 5b). These zircons have uniformly high total REE contents of 3000-6000 ppm (Fig. 5d), Th/U of 1.1 to 1.6, and Ti-in-zircon temperatures of ~800°C (Appendix 4; Watson *et al.*, 2006). The next 5 oldest dates are between 329±5 and 314±6 Ma. These analyses have similar chemical characteristics as the older zircon, and thus likely are part of the same population, with the younger dates being due to slight mixing in the analysis with Jurassic rims. Two analyses of rims yielded a weighted mean of 193±5 Ma (Fig. 5c and Appendix 4). The Jurassic rims have similar CL brightness as the majority of the Mississippian igneous zircon, making it difficult to distinguish the components using CL images alone (Appendix 6). The rims have low total REE contents of ~460 ppm (Fig. 5d), especially light and middle REE contents, and Th/U of 0.03 to 0.25.

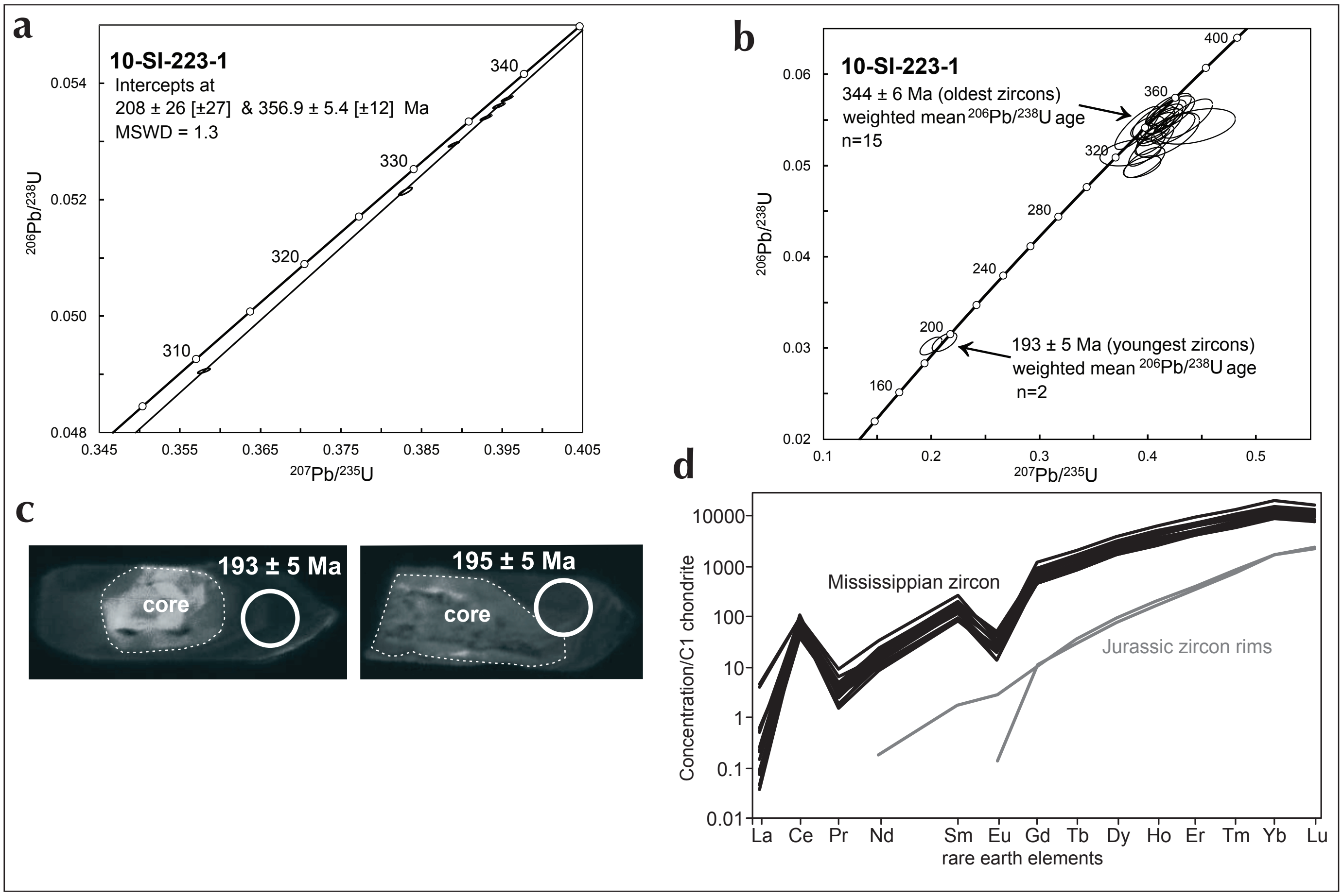

Figure 5. *U-Pb concordia plots for sample 10-SI-223, analyzed at the Isotope Geology Laboratory at Boise State University. (a) concordia plot for CA-TIMS analyses; (b) concordia plot for LA-ICPMS analyses; (c) CL images showing spot yielding Jurassic analyses from zircon rims. Errors are at 2σ. Errors on intercepts defined by CA-TIMS analyses are given without and with U decay constant uncertainties.*

MA14-AB9 – QUARTZ MONZONITE PORPHYRY

MA14-AB9 is a buff-weathering, quartz monzonite porphyry, which contains 35% 2–4 mm K-feldspar phenocrysts and 5% 1–4 mm euhedral to rounded and embayed quartz phenocrysts in a pervasively sericitized quartzofeldspathic groundmass (Fig. 3f). The porphyry forms a recessive topographic saddle between prominent tors of massive, white weathering, coarse-grained, weakly foliated, K-feldspar porphyritic biotite-hornblende granodiorite of the Aishihik batholith west of Buffalo Mountain (Fig. 2).

The 20 zircon grains analyzed by LA-ICPMS were colourless, doubly-terminating prisms with lengths between 100 and 150 µm and with aspect ratios ranging from 2:1 to 4:1. Nineteen of the 20 grains yielded concordant or nearly concordant dates (Fig. 6a and Appendix 5), which, with the exception of one statistically rejected analysis, yielded a weighted average $^{206}Pb/^{238}U$ date of 186 ± 2 Ma (MSWD = 1.5; probability of fit = 0.074).

MA14-AB6 – BIOTITE GRANODIORITE ORTHOGNEISS

MA14-AB6 is a grey, medium-grained biotite granodiorite orthogneiss with a strongly-developed, planar gneissocity, which was collected along the northwest margin of the Aishihik batholith (Figs. 2 and 3h). This flaggy-weathering, outcrop-forming rock has a moderately south-dipping foliation at this locality, and is locally folded about south-plunging axes. Compositional layering ranges from mm-scale biotite-only seams to coarse, granitic layers up to 1-cm thick.

The 19 zircon grains analyzed by LA-ICPMS from the orthogneiss were stubby prisms with lengths between 100 and 150 µm and an average aspect ratio of 1:2. Fifteen of these grains had a colourless and slightly cloudy core with low average CL intensity, rimmed by higher-clarity zircon with higher average CL intensity (Fig. 6b iii-vi). The remaining four zircons imaged contained only the core growth stage. Laser ablation rasters were planned to sample only the core or overgrowth zircon stage with a 25 µm spot. However, where overlap of the two mutually contaminating growth zones was unavoidable, only the portion of the time-series signal that represented a single growth stage was integrated. Seventeen of the 19 analyses represent zircon cores (Fig. 6b iv-vi), whereas in two grains, later stages of zircon overgrowths were sufficiently broad to sample and analyze (Fig. 6b iii-iv).

The 17 analyses of zircon cores fell on or very near to concordia (Fig. 6B iv and Appendix 5), and their weighted average $^{206}Pb/^{238}U$ date is 345 ± 4 Ma (MSWD = 1.5; probability of fit = 0.10). The two analyses of zircon overgrowths were concordant (Fig. 6b i and Appendix 5), and their weighted average $^{206}Pb/^{238}U$ date is 187 ± 5 Ma (MSWD = 0.45; probability of fit = 0.50).

DISCUSSION

The new U-Pb zircon dates reported here generally confirm the age range previously determined by TIMS analyses of multi-grain zircon fractions from samples of the Aishihik batholith (Johnston *et al.*, 1996; Hart, 1997). The SHRIMP dates range from ~190 to ~179 Ma (approximate range including errors; Table 1), with the more mafic rocks (CDB-10-105, 107) yielding older dates (~190-185 Ma), and felsic rocks (CDB-10-102, 103, 106) giving distinctly younger dates of ~184-179 Ma (Fig. 7). This apparently confirms the general field observations suggesting that tonalite-granodiorite phases are older and quartz monzonite-granite phases are relatively younger; although in detail the various phases in the Aishihik batholith appear to be closely related with gradational contacts (Tempelman-Kluit, 1974; Johnston and Erdmer, 1995; Johnston *et al.*, 1996; *this study*). The LA-ICPMS date of 186 ± 2 Ma from a quartz porphyry in the northern part of the Aishihik batholith (MA14-AB9; Fig. 2 and Table 1) is intermediate between the two populations revealed by SHRIMP dates, and may indicate more frequent intrusive episodes leading to batholith construction (Fig. 7). More precise CA-TIMS analyses are required to resolve whether the batholith was constructed from intrusion of two discrete phases or more frequent magma injections.

Johnston and Erdmer (1995) considered the granodiorite-tonalite compositions to be part of the Aishihik plutonic suite (which also included the Granite Mountain, Minto and Tatchun plutons), and the more felsic compositions as belonging to the Long Lake suite (following Tempelman-Kluit, 1974, 1984; Woodsworth *et al.*, 1991). However, the available geochronological dataset (Fig. 7 and Table 1) and the close inter-relations of the various phases in the Aishihik batholith do not warrant division of the batholith into two distinct plutonic suites. We favour assigning granitoid rocks of the Aishihik batholith to the Long Lake suite, ranging from *ca.* 190-180 Ma (Colpron *et al.*, 2016), to avoid potential confusion with recent use of the term Aishihik plutonic suite for older plutons (*see* below).

It is notable that none of the dates obtained from the Aishihik batholith are as old as the *ca.* 204-196 Ma granodiorite of the Granite Mountain, Minto and Tatchun batholiths (Fig. 1; *e.g.*, Tafti, 2005; Hood, 2012; Colpron, 2011; Breistprecher and Mortensen, 2004). These older plutons were previously assigned to the Aishihik suite (*e.g.*, Gordey and Makepeace, 2001) based on their predominantly granodioritic compositions (Johnston and Erdmer, 1995). Because these plutons are distinctly older than any phases dated in the Aishihik batholith, it is recommended that the latest Triassic-Early Jurassic granodiorite plutons that occur mainly north of Carmacks, and host Cu-Au-Ag mineralization at Minto and Carmacks Copper, be assigned to the Minto plutonic suite (*e.g.*, Colpron *et al.*, 2016; Fig. 1). The absence of Minto-age granodiorite in the Aishihik batholith may also suggest lower probability of hosting Minto-style Cu-Au-Ag mineralization in these younger phases.

The range of U-Pb zircon dates from the Aishihik batholith overlaps in part with the range of dated pyroclastic deposits (*ca.* 189-186 Ma; Fig. 7) in the Whitehorse trough, to the east (Nordenskiöld facies, Fig. 2; Colpron and Friedman, 2008). A petrogenetic association between these deposits and the batholith was previously suggested by Hart (1997) and Fillmore (2006). Late Triassic to Early Jurassic plutons of the Minto and Long Lake suites (and their eroded volcanic cover) were also the most significant contributors of detritus in sedimentary rocks of the Whitehorse trough as indicated by abundant plutonic clasts and detrital zircons (Colpron *et al.*, 2015).

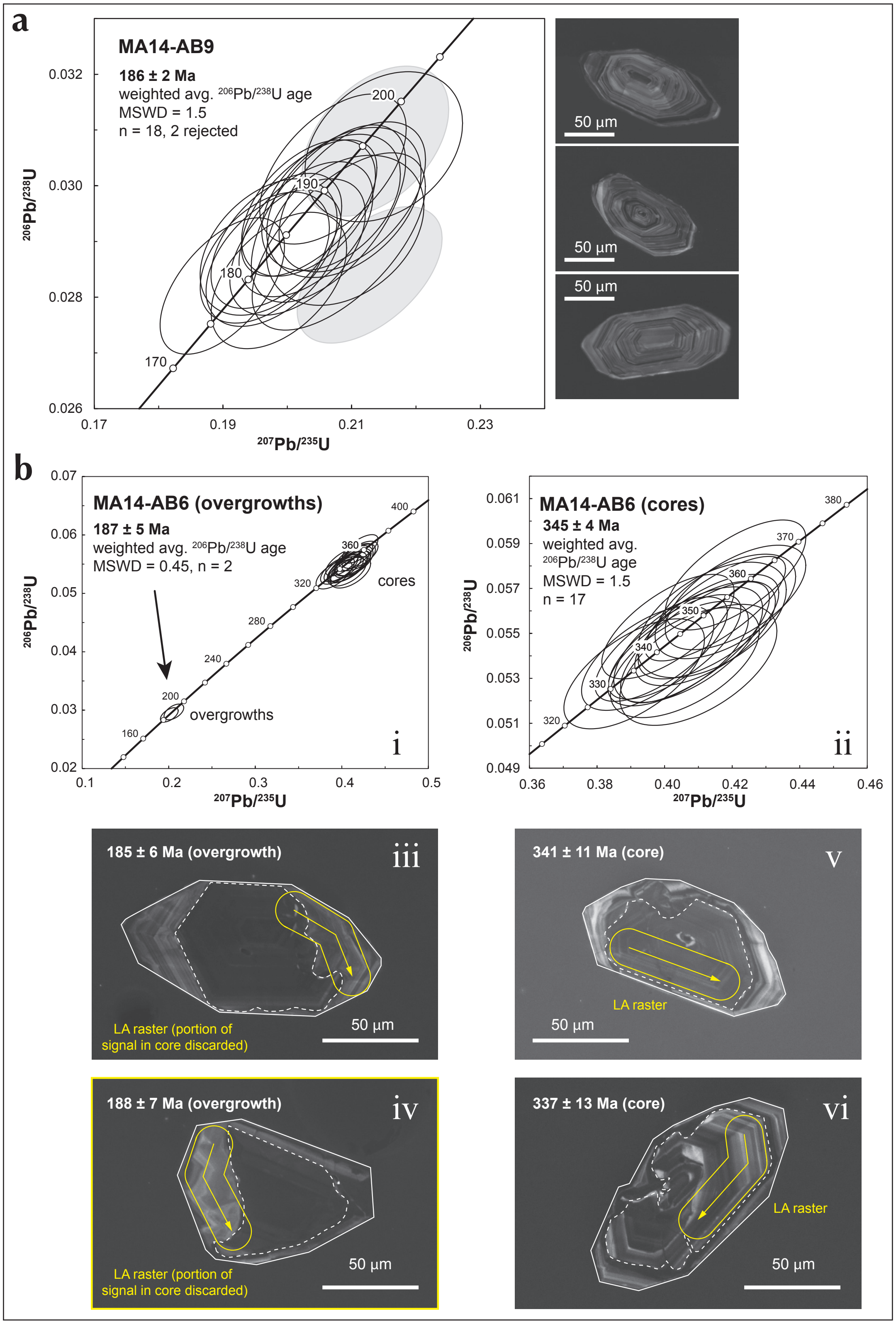

Figure 6. *U-Pb concordia plots for two samples analyzed by LA-ICPMS methods at the Pacific Centre for Isotopic and Geochemical Research at the University of British Columbia. (a) Conventional U-Pb concordia plot for sample MA14-AB9. Error ellipses correspond to 2σ uncertainties in ^{206}Pb/^{238}U and ^{207}Pb/^{235}U ratios. The two rejected analyses have light grey fill. SEM-CL images of three representative, internally zoned zircon grains are shown to the right. (b) Conventional U-Pb concordia plots for zircon from sample MA14-AB6 (i); greater detail of the dominant Early Mississippian population are shown in (ii). Error ellipses correspond to 2σ uncertainties in ^{206}Pb/^{238}U and ^{207}Pb/^{235}U ratios. (iii-iv) SEM-CL images of zircon with Early Jurassic overgrowths; (v-vi) SEM-CL images of zircon with embayed, weakly luminescent, Early Mississippian cores and luminescent overgrowths.*

Previous zircon TIMS analyses from the Aishihik batholith typically yielded discordant dates that resulted in large part as a result of mixing of inherited components and/or post-crystallization Pb loss (Johnston *et al.*, 1996; Hart, 1997). Our new results allow better resolution of inherited versus magmatic components by using a combination of SEM imaging and *in-situ* dating techniques. Inherited cores were identified in 15-25% of zircons imaged with CL SEM (Figs. 4-6). Larger cores were analyzed with the SHRIMP for a few samples (CDB-10-103, 105, 106; Appendix 2). Xenocrystic cores typically reflect interaction with local Paleozoic 'host' rocks (*ca.* 360, 343, 316 and 260 Ma; Yukon-Tanana and/or Stikinia) and older early Mesozoic intrusions (*ca.* 204-196 Ma; Minto suite). A single core was dated at *ca.* 1866 Ma reflecting interaction with either Paleoproterozoic 'basement' or incorporation of a detrital zircon component from metasedimentary rocks of the Yukon-Tanana terrane (Snowcap assemblage; Piercey and Colpron, 2009).

The porphyritic texture in sample MA14-AB9 could be interpreted to indicate it was emplaced at shallower (subvolcanic?) crustal depths, or under H_2O-saturated conditions. Shallow emplacement and/or high volatile content in the magma are also suggested by common occurrences of pegmatite, miarolitic cavities and aplite dikes in the northern part of the batholith. Shallow (<5 km) emplacement of the *ca.* 186 Ma quartz porphyry is unexpected compared to apparently deeper crystallization pressures (3.4-4.2 kbar; ~10-12 km) indicated by Al-in-hornblende analyses of nearby granitic rocks dated at *ca.* 187-183 Ma (CDB-10-106, 107; Fig. 2; Topham *et al.*, 2016). Either this reflects differential exhumation of various parts of the batholith, or the quartz porphyry could be younger than the *ca.* 186 Ma date indicated in Figure 6a. Closer examination of the data in Appendix 5 show a spread of ages between ~196 and ~180 Ma that could represent multiple populations of young zircons (*see* also Fig. 6a). Further analyses using the CA-TIMS method would help improve resolution of these different events. More significantly, the presence of apparently shallower intrusive rocks may indicate potential for porphyry-type Cu-Au mineralization in parts of the Aishihik batholith, especially given that both the Mount Milligan and Lorraine porphyry Cu deposits in northern BC are associated with Early Jurassic intrusions broadly coeval with the Long Lake plutonic suite (Nelson and Bellefontaine, 1996; Jago *et al.*, 2014; Devine *et al.*, 2014; Bath *et al.*, 2014). However, the BC deposits are hosted in alkalic rocks; the Aishihik batholith is generally calc-alkalic to transitional; lithogeochemistry of the Aishihik batholith will be discussed in a future publication.

Two of the samples analyzed in this study are from orthogneiss along the western margin of the Aishihik batholith (10-SI-223 and MA14-AB6; Fig. 2). A previous attempt at dating the orthogneissic rocks along the shore of Aishihik Lake (STJ-OG; Table 1 and Fig. 2) yielded a discordant scatter of zircon analyses suggesting mixing between a predominantly mid-Paleozoic (*ca.* 352 Ma) population of zircons representing the protolith age, and a younger, Mesozoic event of Pb loss or remelting (Johnston *et al.*, 1996). A titanite age of *ca.* 184 Ma provided further constraints on the possible Mesozoic event (Johnston *et al.*, 1996).

CA-TIMS analyses of zircon from orthogneiss at 10-SI-223 yielded a discordant array nearly parallel with concordia, also indicating mixing of mid-Paleozoic and early Mesozoic age components, similar to the sample dated by Johnston *et al.* (1996; Fig. 5a and Appendix 3). LA-ICPMS analysis shows two distinct age clusters, with most zircon being Mississippian (344 ± 6 Ma) and rare rims being Early Jurassic (193 ± 5 Ma; Fig. 5b-c and Appendix 4). LA-ICPMS analysis of another orthogneiss to the north (MA14-AB6; Fig. 2) yielded similar results, with a dominant cluster of older Mississippian zircon (345 ± 4 Ma), and rare Early Jurassic (187 ± 5 Ma) zircon rims (Fig. 6b and Appendix 5). CL images show resorbed Mississippian cores mantled by well-zoned overgrowths (Fig. 6b iii-vi), a pattern that is most consistent with a period of zircon dissolution in a zircon-undersaturated melt, followed by re-precipitation in the presence of a zircon-saturated melt in the Jurassic. Chemical compositions suggest that the Jurassic zircon formed during partial melting of the orthogneiss, rather than crystallizing from a granitoid magma. In both samples, the Jurassic zircon has lower Th/U (0.03-0.25) than typical magmatic zircon (Tables 4 and 5). In sample 10-SI-223, the Jurassic zircon has much lower light and middle REE contents (Fig. 5d) than zircon in typical granitoid magmas. In summary, the zircon textural, age, and chemical data are most consistent with the orthogneiss being an Early Mississippian granitoid of the Simpson Range plutonic suite, which experienced partial melting and ductile strain during emplacement of the Aishihik batholith in the Early Jurassic.

CONCLUSIONS

Five new SHRIMP and one LA-ICPMS U-Pb zircon dates from various granitoid phases in the Aishihik batholith confirm a range of *ca.* 190-180 Ma (Fig. 7); the various phases are all assigned to the Long Lake plutonic suite. Older (*ca.* 204-196 Ma) granodiorite of the Minto suite, host to Cu-Au-Ag mineralization north of Carmacks, appear absent from the Aishihik batholith, but are locally reflected in inherited zircon cores. The Aishihik batholith is therefore an unlikely target for Minto-style mineralization, but local occurrence of apparently shallow-level intrusions in the northern part of the batholith could represent a crustal level permissible for more typical porphyry mineralization. LA-ICPMS U-Pb zircon dating of two orthogneiss samples from the western margin of the Aishihik batholith indicate an Early Mississippian protolith age similar to that of the Simpson Range plutonic suite of Yukon-Tanana terrane. Jurassic overgrowths on several zircon grains indicate an episode of partial melting of the orthogneiss likely related to intrusion of the Aishihik batholith.

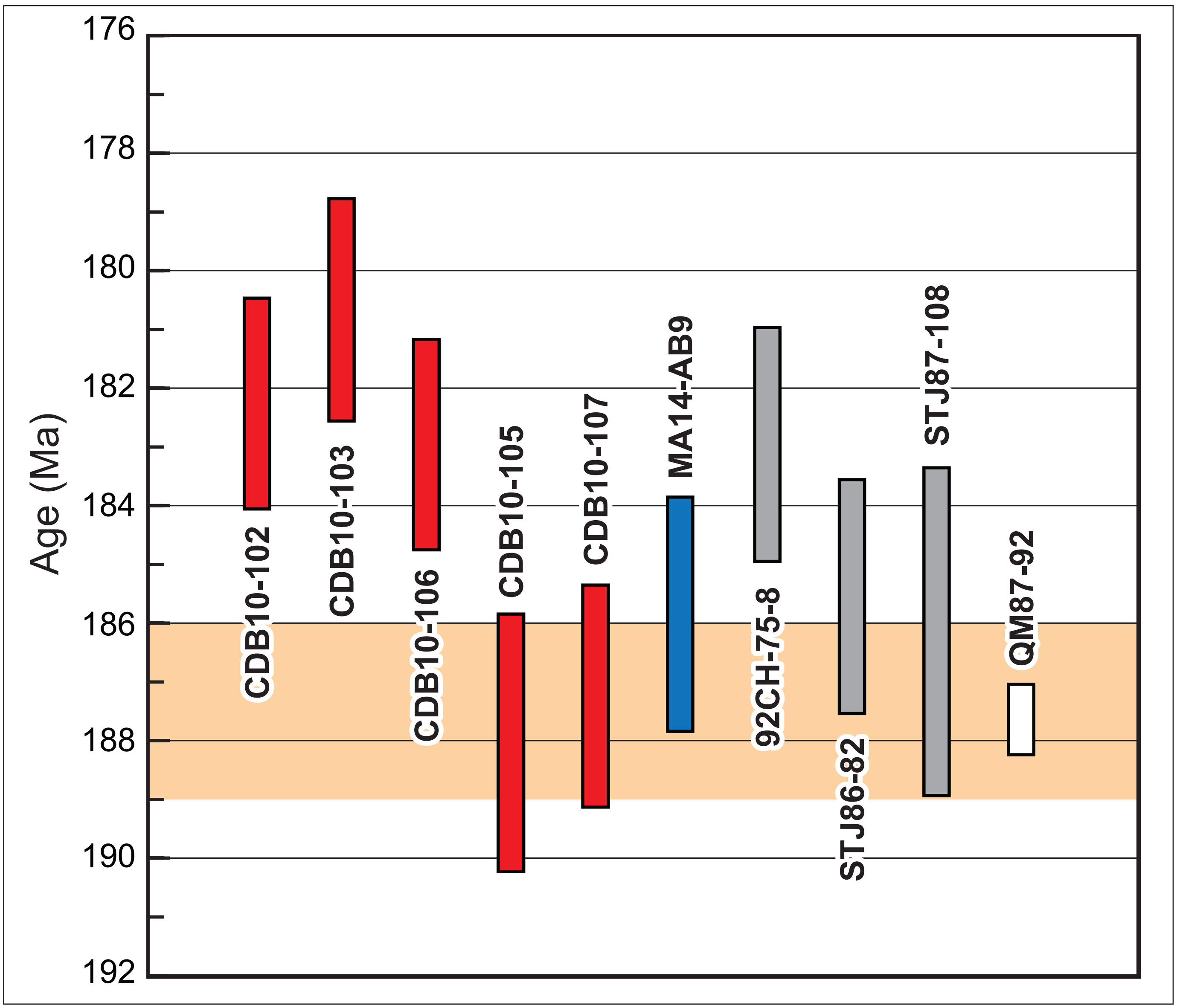

Figure 7. *Summary of U-Pb dates for granitoid samples of the Aishihik batholith (Table 1). Results from orthogneiss samples are omitted. All dates are shown with 2σ errors. Red – SHRIMP zircon date (this study); Blue – LA-ICPMS zircon date (this study); Grey – TIMS multi-grain zircon fractions (Johnston et al., 1996; Hart, 1997); White – TIMS titanite age (Johnston et al., 1996). Orange interval in background indicates the range of dates from pyroclastic rocks in the Whitehorse trough (e.g., Nordenskiöld facies of the Laberge Group; Colpron and Friedman, 2008).*

ACKNOWLEDGMENTS

This study was funded by the Geomapping for Energy and Minerals program of Natural Resources Canada and the Yukon Geological Survey. It is a contribution to the Yukon-Alaska Metallogeny project of the Mineral Deposit Research Unit at the University of British Columbia. Linda Cataldo and Pat Hunt (GSC Ottawa) are thanked for grain mounting and SEM imaging, respectively, for the CDB-10 samples. We thank Tom Pestaj, Bill Davis and Nicole Rayner for their expert guidance and assistance at the GSC SHRIMP facility. Steve Israel collected sample 10-SI-223 and provided the data for this paper. A review by Alex Zagorevski improved the manuscript. This is ESS Contribution number/Numéro de contribution du SST: 20150368.

REFERENCES

Bath, A.B., Cooke, D.R., Friedman, R.M., Faure, K., Kamenetsky, V.S., Tosdal, R.M. and Berry, R.F., 2014. Mineralization, U-Pb geochronology, and stable isotope geochemistry of the lower main zone of the Lorraine deposit, north-central British Columbia: a replacement-style alkalic porphyry. Economic Geology, vol. 109, p. 979-1004,

Breitsprecher, K. and Mortensen, J.K., 2004. Yukonage 2004: A database of isotopic age determinations for rock units from Yukon Territory, Canada. Yukon Geological Survey, Whitehorse, Yukon, www.geology.gov.yk.ca.

Colpron, M., 2011. Geological compilation of Whitehorse trough - Whitehorse (105D), Lake Laberge (105E), and part of Carmacks (115I), Glenlyon (105L), Aishihik Lake (115H), Quiet Lake (105F) and Teslin (105C). Yukon Geological Survey, Geoscience Map 2011-1, scale 1:250 000.

Colpron, M. and Friedman, R. M., 2008. U-Pb zircon ages for the Nordenskiold formation (Laberge Group) and Cretaceous intrusive rocks, Whitehorse trough, Yukon. *In:* Yukon Exploration and Geology 2007, D.S. Emond, L.R. Blackburn, R.P. Hill and L.H. Weston (eds.), Yukon Geological Survey, p. 139-151.

Colpron, M. and Nelson, J.L., 2011. A digital atlas of terranes for the northern Cordillera. Yukon Geological Survey, accessed November, 2015; *also, BC Geological Survey, GeoFile 2011-11*.

Colpron, M., Nelson, J. L. and Murphy, D. C., 2006. A tectonostratigraphic framework for the pericratonic terranes of the northern Canadian Cordillera. *In:* Paleozoic evolution and metallogeny of pericratonic terranes at the ancient margin of North America, Canadian and Alaskan Cordillera, M. Colpron and J.L. Nelson (eds.), Special Paper 45, Geological Association of Canada, p. 1-23.

Colpron, M., Crowley, J.L., Gehrels, G.E., Long, D.G.F., Murphy, D.C., Beranek, L.P. and Bickerton, L., 2015. Birth of the northern Cordilleran orogen, as recorded by detrital zircons in Jurassic synorogenic strata and regional exhumation in Yukon. Lithosphere, vol. 7, p. 541-562.

Colpron, M., Israel, S., Murphy, D.C., Pigage, L.C. and Moynihan, D., 2016. Yukon Bedrock Geology Map 2016. Yukon Geological Survey, Open File 2016-1, scale 1:1 000 000.

Colpron, M., Murphy, D.C., Nelson, J.L., Roots, C.F., Gladwin, K., Gordey, S.P., Abbott, G. and Lipovsky, P.S., 2002. Preliminary geological map of Glenlyon (105L/1-7,11-14) and northeast Carmacks (115I/9,16) areas, Yukon Territory (1:125 000 scale). Exploration and Geological Services Division, Yukon Region, Indian and Northern Affairs Canada, Open File 2002-9, scale; *also Geological Survey of Canada, Open File 1457*.

Devine, F.A.M., Chamberlain, C.M., Davies, A.G.S., Friedman, R.M. and Baxter, P., 2014. Geology and district-scale setting of tilted alkalic porphyry Cu-Au mineralization at the Lorraine deposit, British Columbia. Economic Geology, vol. 109, p. 939-977.

Fillmore, J.A., 2006. Character and origin of the Lower Jurassic (Pleinsbachian) Nordenskiold dacite, Whitehorse trough, Yukon Territory, Canada. Unpublished Honours BSc thesis. Laurentian University, 28 p.

Godwin, C.I., 1975. Alternative interpretations for the Casino complex and Klotassin batholith in the Yukon crystalline terrane. Canadian Journal of Earth Sciences, vol. 12, p. 1910-1916.

Gordey, S.P. and Makepeace, A.J., 2001. Bedrock geology, Yukon Territory. Geological Survey of Canada, Open File 3754, scale 1:1 000 000; *also Yukon Geological Survey, Open File 2001*

Gordey, S.P. and Ryan, J.J., 2005. Geology, Stewart River area (115N, 115O and part of 115J), Yukon Territory. Geological Survey of Canada, Open File 4970, scale 1:250 000.

Gordey, S.P. and Stevens, R.A., 1994. Geology, Teslin, Yukon Territory. Geological Survey of Canada, Open File 2886, scale 1:250 000.

Hart, C.J.R., 1997. A transect across northern Stikinia: Geology of the northern Whitehorse map area, southern Yukon Territory (105D/13-16). Exploration and Geological Services Division, Yukon, Indian and Northern Affairs Canada, Bulletin 8, 112 p.

Hood, S.B., 2012. Mid-crustal Cu-Au mineralization during episodic pluton emplacement, hydrothermal fluid flow, and ductile deformation at the Minto deposit, YT, Canada. Unpublished MSc thesis, University of British Columbia, 220 p.

Israel, S. and Borch, A., 2015. Preliminary geological map of the Long Lake area, parts of NTS 115H/2 and 115H/7. Yukon Geological Survey, Open File 2015-32, 1:50 000 scale.

Jago, C.P., Tosdal, R.M., Cooke, D.R. and Harris, A.C., 2014. Vertical and lateral variation of mineralogy and chemistry in the Early Jurassic Mt. Milligan alkalic porphyry Au-Cu deposit, British Columbia, Canada. Economic Geology, vol. 109, p. 1005-1033,

Johnston, S.T. and Erdmer, P., 1995. Magmatic flow and emplacement foliations in the Early Jurassic Aishihik Batholith, southwest Yukon: Implications for northern Stikinia. *In:* Jurassic Magmatism and Tectonics of the North American Cordillera, D.M. Miller and C. Busby (eds.), Geological Society of America, Special Paper 299, p. 65-82.

Johnston, S.T., Mortensen, J.K. and Erdmer, P., 1996. Igneous and meta-igneous age constraints for the Aishihik metamorphic suite, southwest Yukon. Canadian Journal of Earth Sciences, vol. 33, p. 1543-1555.

Logan, J.M. and Mihalynuk, M.G., 2014. Tectonic controls on Early Mesozoic paired alkaline porphyry deposit belts (Cu-Au ± Ag-Pt-Pd_Mo) within the Canadian Cordillera. Economic Geology, vol. 109, p. 827-858.

Mortensen, J.K., 1992. Pre-Mid-Mesozoic tectonic evolution of the Yukon-Tanana terrane, Yukon and Alaska. Tectonics, vol. 11, p. 836-853.

Nelson, J.L. and Bellefontaine, K.A., 1996. The geology and mineral deposits of north-central Quesnellia: Tezzeron Lake to Discovery Creek, central British Columbia. BC Ministry of Energy, Mines and Petroleum Resources, Bulletin 99, 112 p.

Nelson, J.L., Colpron, M. and Israel, S., 2013. The Cordillera of British Columbia, Yukon, and Alaska: Tectonics and metallogeny. *In:* Tectonics, Metallogeny and Discovery: The North American Cordillera and Similar Accretionary Settings, M. Colpron, T. Bissig, B.G. Rusk and J.F.H. Thompson (eds.), Society of Economic Geologists, Inc., Special Publication 17, p. 53-103.

Piercey, S.J. and Colpron, M., 2009. Composition and provenance of the Snowcap assemblage, basement to the Yukon-Tanana terrane, northern Cordillera: Implications for Cordilleran crustal growth. Geosphere, vol. 5, p. 439-464, doi: 10.1130/GES00505.1.

Tafti, R., 2005. Nature and origin of the Early Jurassic copper (-gold) deposits at Minto and Williams Creek, Carmacks copper belt, western Yukon: examples of deformed porphyry deposits. Unpublished MSc thesis, University of British Columbia, 213 p.

Tempelman-Kluit, D.J., 1974. Reconnaissance geology of Aishihik Lake, Snag and part of Stewart River map-areas, west-central Yukon. Geological Survey of Canada, Paper 73-41, 97 p.

Tempelman-Kluit, D.J., 1984. Geology, Laberge (105E) and Carmacks (105I), Yukon Territory. Geological Survey of Canada, Open File 1101, scale 1:250 000.

Tempelman-Kluit, D.J., 2009. Geology of Carmacks and Laberge map areas, central Yukon: Incomplete draft manuscript on stratigraphy, structure and its early interpretation (*ca.* 1986). Geological Survey of Canada, Open File 5982, 399 p.

Tempelman-Kluit, D.J. and Wanless, R.K., 1975. Porassium-Argon age determinations of metamorphic and plutonic rocks in the Yukon crystalline terrane. Canadian Journal of Earth Sciences, vol. 12, p. 1895-1909.

Topham, M.J., Allan, M.M., Mortensen, J.K., Hart, C.J.R., Colpron, M. and Sack, P.J., 2016. Crustal depth of emplacement of the Early Jurassic Aishihik and Tatchun batholiths, west-central Yukon. *In:* Yukon Exploration and Geology 2015, K.E. MacFarlane and M.G. Nordling (eds.), Yukon Geological Survey, p. 233-251.

Watson, E.B., Wark, D.A. and Thomas, J.B. 2006. Crystallization themometers for zircon and rutile. Contributions to Mineralogy and Petrology, vol. 151, p. 413-433.

Woodsworth, G.J., Anderson, R.G. and Armstrong, R.L., 1991. Plutonic Regimes, Chapter 15. *In:* Geology of the Cordilleran Orogen in Canada, H. Gabrielse and C.J. Yorath (eds.), Geological Survey of Canada, Geology of Canada, no. 4, p. 491-531; *also Geological Society of America, The Geology of North America, vol. G-2*.

APPENDICES

The six appendices for this paper are only available digitally. They are included in a .zip file with this document and available from http://data.geology.gov.yk.ca/.

Appendix 1. Analytical methods

Appendix 2. Data table of all SHRIMP analyses for samples CDB-10-102, 103, 105, 106, 107, analyzed at the Geological Survey of Canada. Bold ^{207}Pb-corrected apparent ages are those used in final weighted mean age calculation, data in italics are rejected from age calculations as discussed in text.

Appendix 3. Data table for CA-TIMS analyses for sample 10-SI-223, analyzed at Boise State University.

Appendix 4. Data table for LA-ICPMS analyses for sample 10-SI-223, analyzed at Boise State University.

Appendix 5. Data table for LA-ICPMS analyses for samples MA14-AB6 and 9, analyzed at the University of British Columbia. Bold ^{206}Pb/^{238}U isotopic ages are those used in final weighted mean age calculation, data in italics are rejected from age calculations as discussed in text.

Appendix 6. CL images of zircon from 10-SI-223. Locations of LA-ICPMS spots are shown with dates in Ma. Spot size is 25 microns. Two analyses of Jurassic rims are shown in yellow. Fraction labels for grains dated by CA-TIMS are shown in red.